

Criteria analysis for kinetics curves of initiated blood serum chemiluminescence

Iryna Oliynyk^{1,2}✉

¹Department of Physical and Chemical Disciplines, Lviv Medical University, Lviv, 79018, Ukraine; ²Institute of Animal Biology of NAAS, Lviv, 79034, Ukraine

The chemiluminescence (CL) methods unlike the other methods of determining free radicals (FR) allow investigating the kinetics of the derivation and recombination of radicals/antioxidants, and thus the development and attenuation of the process/processes after excitation in time. However, these methods are of limited application because the knowledge of the explored parameters is insufficient (maximum intensity and integrated area under the kinetics plot). The kinetics is studied by the CL methods and a new parameter (IR-criterion) of analysis of damping of the initiated CL dynamics has been introduced. The IR-criterion parameter: identifies the relationship between the rates of initiation and recombination of peroxide radicals in blood-serum samples; allows the full straightening of the CL curves; provides new information in the considered pathological processes; can serve as an additional universal characteristic of FR activity of blood serum in pathological processes.

Keywords: chemiluminescence, oxidation, free radicals, kinetics, IR-criteria

Received: 16 April, 2023; **revised:** 11 June, 2023; **accepted:** 16 June, 2023; **available on-line:** 07 September, 2023

✉e-mail: lakmus3041@gmail.com

Abbreviations: CL, chemiluminescence ; BS, blood serum; LPO, lipid peroxidation; FR, free radicals; OS, Oxidative Stress OS

INTRODUCTION

Causal connectivity between pathological states and lipid peroxidation has been analyzed in the scientific literature for a long time and serves as the subject of research by many scientists.

The studies are performed in several directions. Some of them are quantitative content analysis of oxidation products such as diene conjugates and malondialdehyde (Varesi *et al.*, 2022; Eggen *et al.*, 2022; Chen *et al.*, 2022). Other methods include spectral (Rubio *et al.*, 2021) and photometric analysis (Reidy *et al.*, 2023). In this case, one cannot ignore the research methods of the antioxidant status (Bojarczuk *et al.*, 2022), because antioxidants inhibit oxidation processes. All the above-mentioned methods are methods for testing the end-products of oxidation. Only the chemiluminescence methods provide opportunities to study the oxidation dynamics and branching of the oxidation chain (Mas-Bargues *et al.*, 2022). The recombination of radicals R^* , R_2^* leads to light (Damle *et al.*, 2022). The electrons of these substances are in an excited energy level during the transition to the basic state and the substance is emitting the excess energy as a photon. Exactly this emission is called CL (Li *et al.*, 2022). Studying this process can provide much informa-

tion about the processes occurring in the body (Oliynyk 2022).

Considering the benefits of the CL method highlights the following aspects

The first aspect is sensitivity. The recombination of radicals is responsible for the intensity of CL (Romodin 2022; Colowick *et al.*, 1986). Therefore recombination of radicals will determine the intensity of the glow of the process and the presence of oxidative stress (OS) in the body (Colowick *et al.*, 1986) and the CL methods are sensitive. They reveal the influence of drugs on the body and the quality of screening and monitoring therapeutic manipulation (Kohnno *et al.*, 2008).

The second aspect is equally important; it is the speed of analysis. CL analyzers provide information for three minutes, and do not require expensive and specific reagents. In this case, bioliquids analysis as an estimation of the oxidative status of the whole organism is meant, not the surface CL methods of studies of a surface and local detection of problems and areas of defeat (Teruyama *et al.*, 2022; Syed *et al.*, 2021; Deepa *et al.*, 2022).

The usage of luminol and metals of variable valence greatly enhances the potential for utilizing and implementing CL methods in laboratory research. One of the applications is the investigation of the kinetics of initiated CL. The CL kinetics are initiated by adding hydrogen peroxide to the bioliquid, followed by the occurrence of glow kinetics. As with any typical laboratory analysis, such studies should have quantitative characteristics (Freyer *et al.*, 2008). There are several such characteristics identified:

- the intensity of the maximum peak I_{max} – defines the maximum concentration of peroxide radicals formed in the sample after the introduction of hydrogen peroxide;
- the area under the plot S – determines the total number of radicals formed during peroxidation processes.

These are two main features of the study. Also, there are two additional numerical characteristics of kinetics: the maximum angles of the increase and the glow recession. They characterize the maximum rates of formation and recombination of radicals (Oldham *et al.*, 2000; Rizzo *et al.*, 2022; Kaczmarek, 2011; Wang *et al.*, 2016). Yet, all these quantitative characteristics do not allow conducting a qualitative analysis without studying the kinetics curves.

The initial use of the methods of investigation of initiated CL kinetics for the analysis of lipid peroxidation was promising. However, they have not been widely introduced into diagnostic laboratory practice due to some issues:

- the variability of curves of initiated CL
- these parameters (I_{max} , S) do not allow a quantitative diagnosis of pathology (Muller *et al.*, 2013)
- at pathological stages, these parameters often overlap
- deviation of one of them does not always indicate pathology
- getting two or more parameters in normal limits does not ensure the absence of a pathological condition.

The present article is devoted to the finding of such an additional quantitative clinical diagnostic criterion for analyzing initiated CL kinetics.

MATERIALS AND METHODS

The method of initiated CL requires using $FeSO_4$ to study blood serum. Ions of variable valence make it possible to increase the intensity of CL by oxidation chain branching. The temperature of the experiment was 38°C.

In experiments, we used fibrinogen-free BS of healthy people and also patients with different pathological processes. Blood samples for the experiments were taken in the morning on an empty stomach. The initiated H_2O_2 (2%) CL BS in the solution (BS + $FeSO_4$) (0.02 mM) + phosphate buffer) was investigated. We did not utilize any additional radiation to initiate the luminescence. The glow resulting from the chemical reaction was captured using an FEU-79 photomultiplier. The electrical signal obtained was then amplified and processed by a PC (refer to Fig. 1).

More details on the experiment methodology and equipment are available below in this article (Oliynyk, 2016; Chaichi *et al.*, 2016).

Free radical oxidation involves three stages: initiation with speed w_i , propagation, and termination (free radicals combine to form stable molecules (with radiation of excess energy) and prevent their further reaction with other molecules (without light emission)).

Overall, free radical oxidation can cause damage to cells and tissues in the body, leading to various diseases and conditions such as cancer, cardiovascular disease, and aging. Antioxidants can help to prevent or reduce the damage caused by free radicals by neutralizing them and breaking the chain reaction.

The most significant influence on the CL process with a lack of branching is introduced by the recombination of radicals. Consequently, the emission intensity is proportionate to the speed of that recombination:

$$I = \eta k [\text{radicals}]^2 \quad (1)$$

where:

η – the CL quantum efficiency

k – the constant of the speed of the peroxy radicals recombination

$[\text{radicals}]$ – the radicals concentration.

Since the recombination of FR mainly leads to radiation. Initiation is characterized by a sharp flash, and transition into the stationary condition is characterized by a decrease in the CL intensity.

In Non-Stationary mode:

$$-\frac{d[\text{radicals}]}{dt} = w_i - \eta k [\text{radicals}]^2 \quad (2)$$

where w_i is the constant of the rate of the radicals formation.

t – time moment.

We ignored all the intermediate reactions of peroxidation therefore in the future we will use the above definition.

Integration of the given formula leads to the following result:

$$\frac{1}{2\sqrt{w_i k}} \ln \frac{[\text{radicals}]\sqrt{k} + \sqrt{w_i}}{[\text{radicals}]\sqrt{k} - \sqrt{w_i}} = t \quad (3)$$

In Stationary mode, when our system stabilizes $\frac{d[\text{radicals}]}{dt} = 0$, so:

$$[\text{radicals}]_{\infty} = \sqrt{\frac{w_i}{k}} \quad (4)$$

then we get

$$\ln \frac{[\text{radicals}] + [\text{radicals}]_{\infty}}{[\text{radicals}] - [\text{radicals}]_{\infty}} = 2t\sqrt{w_i k} \quad (5)$$

substitute into (see Eqn 5):

$$\frac{I_{\infty}}{I} = \frac{[\text{radicals}]_{\infty}^2}{[\text{radicals}]^2} \quad (6)$$

the final result:

$$\ln \frac{\sqrt{I} + \sqrt{I_{\infty}}}{\sqrt{I} - \sqrt{I_{\infty}}} = 2t\sqrt{w_i k} \quad (7)$$

where:

– the time from the moment when hydrogen peroxide was introduced

I – the emission intensity for the t time moment

I_{∞} – the emission intensity at the moment when intensity becomes stationary (in our case after 70 seconds).

So in $(t, \ln \frac{\sqrt{I} + \sqrt{I_{\infty}}}{\sqrt{I} - \sqrt{I_{\infty}}})$, rectification of the initiated CL kinetics coordinates should take place.

BS is a complex heterogeneous environment and therefore the process of oxidation and recombination will be much more difficult for several reasons. Primarily, the heterogeneity and presence processes of radical hydration radicals. This will be shown in forthcoming studies on spectrum analysis during the reaction of recombination of peroxide radicals.

Note that the kinetics of fluorescence and phosphorescence spectra often exhibit similar kinetic curves. However, in the case of chemiluminescence, the glow occurs due to the recombination of free radicals, such as peroxides, which are formed as a result of a chemical reaction. The subsequent process involves relaxation to the ground state of the recombination products. In contrast, in fluorescence and phosphorescence kinetics (without observing a

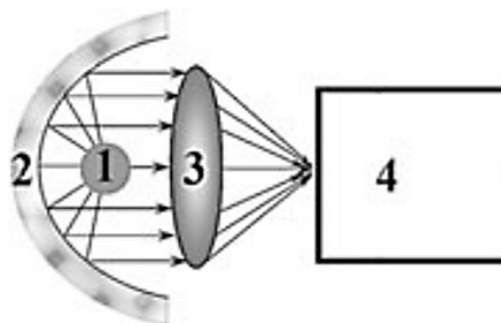


Figure 1. Chemiluminometer.

1: Suvette with the sample; 2: Parabolic mirror; 3: Collective lens; 4: Photodetector device, which includes a system of detection, amplification, conversion, analysis and signal output.

chemical reaction), only relaxation to the ground state occurs, as the molecule is excited during light irradiation of the sample. If fluorescence and phosphorescence are utilized to enhance the glow in the chemiluminescence reaction, the proposed approach carries the same significance.

All the samples of BS at pathological conditions were taken before medical treatment. The main task of this study is to refute or confirm the theory that chemiluminograms will be straightened in the specified coordinates. That the tangent of the straightening angle (IR-criterion) may vary depending on the pathology.

More than 774 chemiluminograms were analyzed, but only a few pathological conditions were selected. The criterion for choosing pathological conditions to be analyzed was an attempt to combine viral, bacterial, and fungal infections, and diseases of unknown etiology – sarcoidosis. We did not include cancer – they will be the subject of a forthcoming study.

Note: On each BS sample, we conducted a minimum of three independent parallel experiments and made an interesting discovery. When it came to I_{\max} and S , we had to discard results that deviated by more than 5% to avoid false-positive outcomes. However, for the angle tangent, such exclusion was unnecessary as the results did not differ by more than 5%. Thus, the relationship between the rates of initiation and recombination of peroxide radicals in the samples appears to be a more stable characteristic than the area under the plot and the maximum intensity of ICL. This suggests that in the analysis of $2\sqrt{w_i k}$, we have a more reliable parameter than I_{\max} and S . Nonetheless, chemiluminograms displaying a deviation of more than 5% across all these parameters were rejected since we also analyzed the average values for I_{\max} and S . Please refer to Fig. 2 for the calculation scheme.

Below we describe the division of patients suffering from different forms and diseases into six groups:

1. Active forms of pulmonary tuberculosis 14 (fourteen) people, the tuberculosis was diagnosed for the first time (disseminated forms of tuberculosis).
2. Sarcoidosis 8 (eight) people.
3. Hepatitis 21 (twenty-one) people. Viral hepatitis is not divided into subgroups. The group includes viral hepatitis of the group A, B, C.
4. Influenza 20 (twenty) people. The blood sampling was done after hospitalizing, the strain was not classified.
5. Asperhiloma 5 (five) people. Asperhiloma of the lungs was investigated against the background of pulmonary tuberculosis.
6. The control group of 51 (fifty-one) people.

RESULTS AND DISCUSSION

The differences in the results for I_{\max} and S between the control group and pathological conditions were not

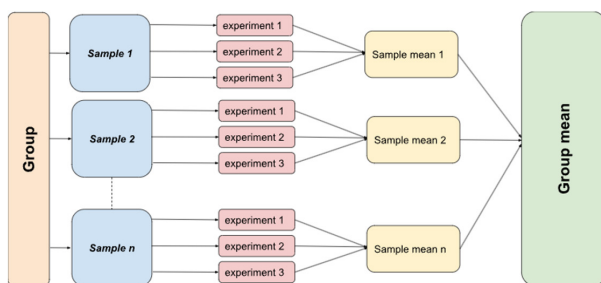


Figure 2. Scheme of conducting experiments and calculations in each group.

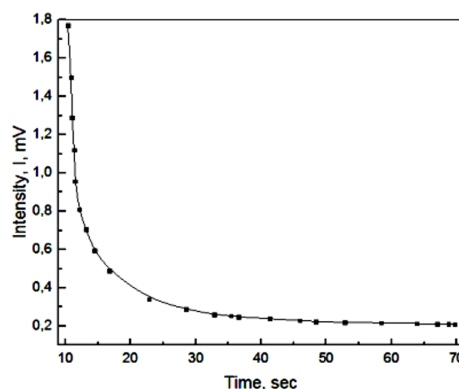


Figure 3. Typical view of a chemiluminogram of one of the samples of the control group.

always clear although these parameters were well correlated between themselves within a group.

The group correlation coefficients:

1. Active forms of pulmonary tuberculosis – 0.944
2. Sarcoidosis – 0.88
3. Hepatitis – 0.84
4. Influenza – 0.95
5. Asperhiloma – 0.76
6. Control – 0.93.

This means that within a group the parameters I_{\max} and S are interrelated. The weakest correlation between I_{\max} and S values was observed in aspergilloma. This could be due to the fungal infection and its stage, which can cause changes in the ratio between primary and secondary radicals in the middle of the group. Similar deviations were also observed in the middle of the group with sarcoidosis and hepatitis. Chemiluminescence is a highly sensitive parameter, and even the phase of the lesion can affect the relationship between I_{\max} and S values, and thus the correlation between them.

Figure 3 shows a typical view of a chemiluminogram of one of the samples of the control group. The first maximum appeared at 0.6–1 sec after the introduction of H_2O_2 . After this, the intensity of luminescence sharply decreased.

In the control group and in all pathological processes, there was no difference in the chemiluminogram view (except the group of chemiluminograms for certain types of cancer). All the chemiluminograms have an exponential character.

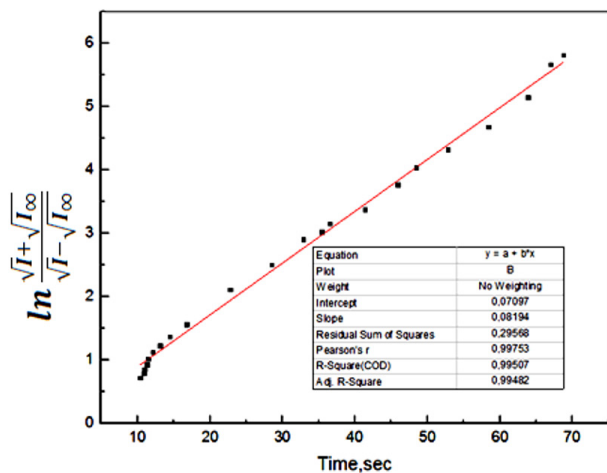
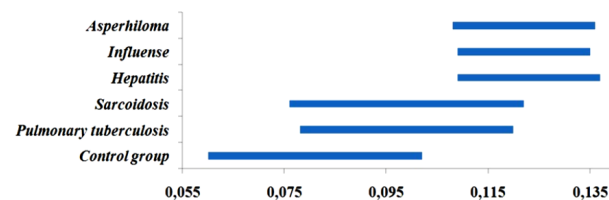
The confidence intervals of the main parameters for each pathology (the maximum intensity and the area under the plot) overlap with the confidence intervals of the parameters for the control group. This indicates selective sensitivity to the disease and low specificity of the corresponding criteria (see Table 1).

The analysis of chemiluminograms as to the coordinates $(t; \ln \frac{\sqrt{t} + \sqrt{t_0}}{\sqrt{t} - \sqrt{t_0}})$ (see Fig. 4) showed the straightening of chemiluminograms for the control group and in all pathological conditions in coordinates $(t; \ln \frac{\sqrt{t} + \sqrt{t_0}}{\sqrt{t} - \sqrt{t_0}})$.

Let's write the equation $\ln \frac{\sqrt{t} + \sqrt{t_0}}{\sqrt{t} - \sqrt{t_0}} = 2t\sqrt{w_i k}$ in the form $y=at$, where $y = \ln \frac{\sqrt{t} + \sqrt{t_0}}{\sqrt{t} - \sqrt{t_0}}$. The coefficient for the variable (angle coefficient) $a = 2\sqrt{w_i k}$, is nothing but the tangent of the angle of inclination of the straight line to the abscissa axis. The $2\sqrt{w_i k}$ (IR-criterion) differs from the control group under pathological conditions. Note that we have not analyzed chemiluminograms of other biological fluids; the obtained results we can design only for the blood serum tests (Table 1).

Table 1. Average measured values for different groups.

Pathological conditions	$I_{\max} \pm m$ (mV)	$S \pm m$ (mV*sec)	IR-criterion $\pm m$
Control group	1.76 \pm 0.07	18.91 \pm 1.21	0.081 \pm 0.021
Pulmonary tuberculosis	3.10 \pm 0.59	38.42 \pm 4.69	0.099 \pm 0.021
Sarcoidosis	2.72 \pm 0.57	46.98 \pm 3.85	0.099 \pm 0.023
Hepatitis	2.154 \pm 0.34	28.45 \pm 2.18	0.123 \pm 0.014
Influenza	1.946 \pm 0.37	23.84 \pm 2.22	0.122 \pm 0.013
Asperhiloma	0.677 \pm 0.08	12.73 \pm 1.14	0.122 \pm 0.014

Figure 4. Dependence of $\ln \frac{\sqrt{I} + \sqrt{I_{\infty}}}{\sqrt{I} - \sqrt{I_{\infty}}}$ on the time for the ICL curves.Figure 5. The confidence intervals of parameter $2\sqrt{w_i k_6}$.

A significant increase in the parameters I_{\max} and S relative to the control group was observed only in groups 1 (tuberculosis) (I_{\max} at 76.14% ($p < 0.05$), S at 103.17% ($p < 0.01$)) and 2 (sarcoidosis) (I_{\max} at 54.55% ($p < 0.05$), S at 147.17% ($p < 0.01$)). Such an increase indicates a significant increase of FR in the organism. We know that a quick flash is responsible for the number of primary FR formed in the organism. The primary radicals include semihions, superoxides, and nitroxides. The FR formed during the oxidation are consumed by recombination with emissions of light. Note that under the introduction of hydrogen peroxide into the samples, in the control group and in all pathologies, it was observed a significant level of CL 0.05–0.08 mV. When we came to the plateau of chemiluminograms (in the simulation, we considered this level as a steady state), this level was higher than the original level – 0.1–0.7 mV. The secondary oxidation processes that occur in the system correspond to this level. The high level of the plateau at tuberculosis and sarcoidosis indicates the significant number of secondary radicals formed in the serum samples. These radicals include hypochloride, hydroxyl radicals, and lipid radicals. The parameter S which indicates

the total number of recombinant radicals in the sample by eliminating the quanta of light is also much higher than the norm.

A large number of primary radicals is also observed with diseases such as hepatitis and influenza. $I_{\max} = 2.154$ mV – at hepatitis and 1.946 mV – at influenza, however, the situation changes when we consider the total number of radicals recombined by light emission («Hepatitis» $S = 28.45$ mV \times sec, «Influence» $S = 23.84$ mV \times sec). At the same time, under these pathologies we sometimes observed results falling into the normal range on these parameters.

A totally different case was with tuberculosis complicated by asperhiloma. In this case, both the number of primary radicals and secondary radicals recombined by light emission was below the norm. These effects can be caused by the four ways of reaction evolution in the sample:

1. the low level of radicals;
2. the high level of antioxidants;
3. non-radiative recombination of radicals;
4. the luminescence quenching molecules' environment.

All these four ways and mechanisms are equally possible and require further study.

The results for the angles tangents of straightening are not homogeneous. In particular – in the IR-criterion, no significant increase in tuberculosis and sarcoidosis was observed. Also, there is an overlapping of the confidence intervals in these diseases (Fig. 5).

A significant overlap of the confidence intervals is observed between tuberculosis and control groups ($p > 0.75$), and between the sarcoidosis and control groups ($p > 0.75$). At the same time, no overlapping of confidence intervals at hepatitis ($p < 0.01$), influenza ($p < 0.01$), and asperhiloma ($p < 0.01$) were found.

A significant and sustained increase of IR-criteria at influenza, hepatitis, and asperhiloma was observed, which indicates that in these diseases deviations towards the initiation/recombination of peroxide radicals occur. So, we can confidently apply this parameter as an additional criterion to improve chemiluminogram analysis in various pathological conditions, as well as the investigation of processes of free radical oxidation (FRO) and OS.

In modern biology, the activation of lipid peroxidation is considered a universal response of living systems to extreme factors. In general, the prooxidant-antioxidant status of the organism reflects the balance between the two opposite actions, namely the antioxidant properties (defence) and the formation of FR (damage). The influence of extreme factors (viruses, bacteria, xenobiotics, radiation, etc.) leads to the rejection of their balance in the prooxidant direction and the development of the so-called OS (Paulsen *et al.*, 2013). On the one hand, FRO at all stages of the course forms a series of products re-

sulting from the interaction of FR with each other and with biological macromolecules (Rahman, 2013). On the other hand, the analysis of the kinetic profile has not appeared as a universal factor in the process progress analysis. Important is the fact that the results of our investigation comply with the data published in literary sources. For example, the authors in (Wilson *et al.*, 2009) point to the fact that the FR play a significant role in the formation of lung fibrosis in pulmonary tuberculosis. This is confirmed by our results, in particular, we observed the increased levels of FR which caused an increase in both CL intensity maximum and S parameter.

For tuberculosis, the rate constants of initiation-recombination reactions are slightly different from the norm. Pulmonary tuberculosis is a serious and contagious illness that results from infection with *Mycobacterium tuberculosis*. It was studied in research the levels of free radicals, antioxidant capacity, and lipid profile in individuals who are afflicted with pulmonary tuberculosis (Vidhya *et al.*, 2019). When macrophages engulf *Mycobacterium tuberculosis*, the bacterium prevents the phagosome from maturing and fusing with lysosomes. This allows the pathogen to survive and multiply inside the phagocytic vacuoles, despite the hostile environment created by reactive oxygen and nitrogen intermediates produced by the macrophages. These highly toxic molecules, which include hydrogen peroxide, nitric oxide, and peroxytrite, are normally produced at low levels during metabolic processes and are neutralized by antioxidant systems in the cell. However, during infection, their concentrations increase and cause damage to the cell's lipids, nucleic acids, proteins, and metal cofactors, leading to mutagenesis, necrosis, and apoptosis (Dalvi *et al.*, 2013) This may be due to a proportional increase in both the primary and secondary FR (Meulmeester *et al.*, 2022) in the body.

Sarcoidosis also causes the OS. Our results reflect an increase of the same parameters (I_{max} and S), therefore the content of FR. Other authors (Boots *et al.*, 2009) point to the reduction of the blood serum antioxidant status. The dependence of the rate of initiation of oxidation and recombination of radicals in this case has not changed, therefore the ratio of primary and secondary radicals in this case corresponds to the norm.

Hepatitis has slightly different parameters. The significantly increased level ($2\sqrt{w_i k}$) of primary radicals against the background of reducing the secondary oxidation processes reveals the fact that the virus itself induces reactive forms of oxygen (Farinati *et al.*, 2007). So, we can predict an increase in oxidation rate constants of oxidation initiation. Furthermore, the mitochondrial dysfunction, observed in work (Moezzi *et al.*, 2022), is induced by the hepatitis C virus and decreases the oxidation of fat acids and accelerates the formation of reactive oxygen forms causing fat accumulation in the liver. This indicates that the number of secondary radicals is reduced, as well as the total number of FR, which fully confirms our results.

Influenza is also characterized by increasing of primary radicals against the background of reducing the total number of radicals in the organism. The indicator IR-criterion increased at this pathological state to which we also find the confirmation in the literature. In particular, in (Andrés *et al.*, 2022), the increase in reactive oxygen forms under this pathological condition was emphasized.

Asperhiloma was the last interesting subject of our study. Again, we observed a decrease in both primary and secondary radicals. Literature source (Ryoo *et al.*, 2009) provides an interesting fact concerning the synthe-

sis of connections based on the fermentation broth of *Aspergillus sp.* FN070449 (KCTC 26428) with antioxidant properties. So, the aspergillus infection as a complication of tuberculosis may lead to a reduction of the total number of FR. But at the same time, it increases relative to the control group, that is the ratio of primary and secondary radicals increases. The above considerations prove, that the introduced criterion, quantitatively and informatively shows the evolution of oxidative processes in the organism and can serve as an additional clinical diagnostic criterion for the quantitative analysis of chemiluminograms.

Although the analysis of chemiluminograms did not demonstrate selective specificity and sensitivity towards pathologies, it is still a useful and relevant method for evaluating the level of free radical processes in patients and monitoring their dynamics (for the purpose of assessing treatment effectiveness). Additional justification is required for the analysis of fluorescence and phosphorescence kinetics. However, preliminary analysis suggests that the fluorescence and phosphorescence kinetic curves also align within these coordinates.

CONCLUSIONS

As a result of the analysis of chemiluminograms, we introduced an additional quantitative criterion (IR-criteria/ $2\sqrt{w_i k}$). The parameter introduced displays the angle tangent of straightening chemiluminograms in the coordinates ($t; \ln \frac{\sqrt{t+I_{max}}}{\sqrt{t-I_{min}}}$). This straightening was observed in

chemiluminograms under normal conditions and in pathological processes, with the exception of with the exception of chemiluminograms characterized by two peaks. The basic assumption in the simulation was the absence of a degenerate chain FRO.

Through a comparative analysis of available publications, we found significant consistency between the data of peroxide oxidation/free radicals and obtained by us the new parameter. This suggests that this criterion can be considered a complementary and independent parameter for estimating FRO.

Therefore, the investigation of the straightening of chemiluminograms in the coordinates ($t; \ln \frac{\sqrt{t+I_{max}}}{\sqrt{t-I_{min}}}$) reveals promising perspectives for comparative monitoring of pathological states and creates a new paradigm in the study of the kinetics of initiated CL. This analysis will enable the combination of parameters such as intensity and area under the graph, providing an additional description of the rapid chemical transformations accompanied by light emission.

REFERENCES

- Andrés CMC, Pérez de la Lastra JM, Juan CA, Plou FJ, Pérez-Lebeña E (2022) The role of reactive species on innate immunity. *Vaccines* **10**: 1735. <https://doi.org/10.3390/vaccines10101735>
- Bojarczuk A, Dzitkowska-Zabielska M (2022) Polyphenol supplementation and antioxidant status in athletes: a narrative review. *Nutrients* **15**: 158. <https://doi.org/10.3390/nu15010158>
- Boots AW, Drent M, Swennen EL, Moonen HJ, Bast A, Haenen GR (2009) Antioxidant status associated with inflammation in sarcoidosis: a potential role for antioxidants. *Respir Med* **103**: 364–372. <https://doi.org/10.1016/j.rmed.2008.10.007>
- Chaichi MJ, Ehsani M. (2016) A novel glucose sensor based on immobilization of glucose oxidase on the chitosan-coated Fe₃O₄ nanoparticles and the luminol-H₂O₂-gold nanoparticle chemiluminescence detection system. *Sensors Actuators B-Chem* **223**: 713–722. <https://doi.org/10.1016/j.SNB.2015.09.125>
- Chen HC, Chen CY, Fang YH, Hung KW, Wu DC (2022) Malondialdehyde-induced post-translational modifications in hemoglobin of

- smokers by NanoLC-NSI/MS/MS analysis. *J Proteome Res* **21**: 2947–2957. <https://doi.org/10.1021/acs.jproteome.2c00442>
- Colowick NP, Kaplan NP (1986) Bioluminescence and chemiluminescence. (1986) *Methods Enzymol Part B*. **133**: 1–649
- Dalvi SM, Patil VW, Ramraje NN, Phadtare JM, Gujarathi SU (2013) Nitric oxide, carbonyl protein, lipid peroxidation and correlation between antioxidant vitamins in different categories of pulmonary and extra pulmonary tuberculosis. *Malaysian J Med Sci* **20**: 21–30
- Damle VG, Wu K, Arouri DJ, Schirhagl R. (2022) Detecting free radicals post viral infections. *Free Radic Biol Med* **191**: 8–23. <https://doi.org/10.1016/j.freeradbiomed.2022.08.013>
- Deepa S, Ramu A, Rajendrakumar K (2022) Natural catalyst for luminol chemiluminescence: application to validate peroxide levels in commercial hair dyes. *Luminescence* **37**: 558–568. <https://doi.org/10.1002/bio.4182>
- Eggen MD, Merboth P, Neukirchner H, Glomb MA (2022) Lipid peroxidation has major impact on malondialdehyde-derived but only minor influence on glyoxal and methylglyoxal-derived protein modifications in carbohydrate-rich foods. *J Agric Food Chem* **70**: 10271–10283. <https://doi.org/10.1021/acs.jafc.2c04052>
- Farinati F, Cardin R, Bortolami M, Burra P, Russo FP, Rugge M, Guido M, Sergio A, Naccarato R (2007) Hepatitis C virus: from oxygen free radicals to hepatocellular carcinoma. *J Viral Hepatitis* **14**: 821–829. <https://doi.org/10.1111/j.1365-2893.2007.00878.x>
- Freyer W, Neacsu CC, and Raschke MB (2008) Absorption, luminescence, and Raman spectroscopic properties of thin films of benzoannulated metal-free porphyrazines. *J Lumines* **128**: 661–672. <https://doi.org/10.1016/j.jlum.2007.11.070>
- Kaczmarek M (2011) Chemiluminescence of the reaction system Ce(IV)-non-steroidal anti-inflammatory drugs containing europium(III) ions and its application to the determination of naproxen in pharmaceutical preparations and urine. *J Fluorescence* **21**: 2201–2205. <https://doi.org/10.1007/s10895-011-0923-2>
- Kohno M, Takeda M, Nivano Y, Saito R, Emoto N, Tada M, Kanazawa T, Ohuchi N, Yamada R (2008) Early diagnosis of cancer by detecting the chemiluminescence of hematoporphyrins in peripheral blood lymphocytes. *Toboku J Exp Med* **216**: 47–52. <https://doi.org/10.1620/tjem.216.47>
- Li M, Jiang R, Wang E, Xiong D, Ou T, Zhang X, Dou X. (2022) Performance evaluation of an automatic chemiluminescence immune platform for SARS-CoV-2 neutralizing antibody after vaccination in real world. *BMC Infect Dis* **22**: 157. <https://doi.org/10.1186/s12879-022-07141-8>
- Mas-Bargues C, García-Domínguez E, Borrás C (2022) Recent approaches to determine static and dynamic redox state-related parameters. *Antioxidants (Basel, Switzerland)* **11**: 864. <https://doi.org/10.3390/antiox11050864>
- Meulmeester FL, Luo J, Martens LG, Mills K, van Heemst D, Noordam R (2022) Antioxidant supplementation in oxidative stress-related diseases: what have we learned from studies on alpha-tocopherol?. *Antioxidants (Basel, Switzerland)* **11**: 2322. <https://doi.org/10.3390/antiox11122322>
- Moezzi D, Dong Y, Jain RW, Lozinski BM, Ghorbani S, D'Mello C, Wee Yong V (2022) Expression of antioxidant enzymes in lesions of multiple sclerosis and its models. *Sci Rep* **12**: 12761. <https://doi.org/10.1038/s41598-022-16840-w>
- Muller C H, Lee TK, Montañó MA (2013). Improved chemiluminescence assay for measuring antioxidant capacity of seminal plasma. *Methods Mol Biol* **927**: 363–376. https://doi.org/10.1007/978-1-62703-038-0_31
- Oldham PB, McCarroll ME, McGown LB, Warner IM. (2000). Molecular fluorescence, phosphorescence, and chemiluminescence spectrometry. *Anal Chem* **72**: 197R–209R. <https://doi.org/10.1021/a1000017p>
- Oliynyk I (2016) Limits of application of initiated chemiluminescence in monitoring of oncological process of mucous membrane of mouth and larynx. *Luminescence* **31**: 1213–1219. <https://doi.org/10.1002/bio.3093>
- Paulsen CE, Carroll KS (2013) Cysteine-mediated redox signaling: chemistry, biology, and tools for discovery. *Chem Rev* **113**: 4633–4679. <https://doi.org/10.1021/cr300163e>
- Rahman K (2007). Studies on free radicals, antioxidants, and co-factors. *Clin Intervent Aging* **2**: 219–236
- Reidy E, Bottorff BP, Rosales CMF, Cardoso-Saldaña FJ, Arata C, Zhou S, Wang C, Abeleira A, Hildebrandt Ruiz L, Goldstein AH, Novoselac A, Kahan TF, Abbott JPD, Vance ME, Farmer DK, Stevens PS (2023) Measurements of hydroxyl radical concentrations during indoor cooking events: evidence of an unmeasured photolytic source of radicals. *Environ Sci Technol* **57**: 896–908. <https://doi.org/10.1021/acs.est.2c05756>
- Rizzo F (2022) Optical immunoassays methods in protein analysis: an overview. *Chemosensors* **10**: 326. <https://doi.org/10.3390/chemosensors10080326>
- Romodín LA (2022) Chemiluminescence detection in the study of free-radical reactions. Part 2. Luminescent additives that increase the chemiluminescence quantum yield. *Acta Naturae* **14**: 31–39. <https://doi.org/10.32607/actanaturae.11427>
- Rubio CP, Cerón JJ (2021) Spectrophotometric assays for evaluation of Reactive Oxygen Species (ROS) in serum: general concepts and applications in dogs and humans. *BMC Vet Res* **17**: 226. <https://doi.org/10.1186/s12917-021-02924-8>
- Ryoo IJ, Xu GH, Kim YH, Choo SJ, Ahn JS, Bae K, Yoo ID (2009) Reticulone, a novel free radical scavenger produced by *Aspergillus* sp. *J Microbiol Biotechnol* **19**: 1573–1575. <https://doi.org/10.4014/jmb.0906.06033>
- Syed AJ, Anderson JC (2021) Applications of bioluminescence in biotechnology and beyond. *Chem Soc Rev* **50**: 5668–5705. <https://doi.org/10.1039/d0cs01492c>
- Teruyama K, Naruse M, Tsuiji M, Kobayashi H (2022) Novel chemiluminescent immunoassay to measure plasma aldosterone and plasma active renin concentrations for the diagnosis of primary aldosteronism. *J Hum Hypertens* **36**: 77–85. <https://doi.org/10.1038/s41371-020-00465-5>
- Varesi A, Chirumbolo S, Campagnoli LIM, Pierella E, Piccini GB, Carrara A, Ricevuti G, Scassellati C, Bonvicini C, Pascale A (2022) The role of antioxidants in the interplay between oxidative stress and senescence. *Antioxidants (Basel, Switzerland)* **11**: 1224. <https://doi.org/10.3390/antiox11071224>
- Vidhya, R., Rathnakumar, K., Balu, V., Pugalendi, K. V. (2019). Oxidative stress, antioxidant status and lipid profile in pulmonary tuberculosis patients before and after anti-tubercular therapy. *Indian J Tuberc* **66**: 375–381. <https://doi.org/10.1016/j.ijtb.2018.11.002>
- Wang C, Zhou C, Long Y, Cai H, Yin C, Yang Q, Xiao D (2016). An enhanced chemiluminescence bioplatfrom by confining glucose oxidase in hollow calcium carbonate particles. *Sci Rep* **6**: 24490. <https://doi.org/10.1038/srep24490>
- Wilson MS, Wynn TA (2009) Pulmonary fibrosis: pathogenesis, etiology and regulation. *Mucosal Immunol* **2**: 103–121. <https://doi.org/10.1038/mi.2008.8>